Toxicology Reports 6 (2019) 768–781

Contents lists available at ScienceDirect

Toxicology Reports

journal homepage: www.elsevier.com/locate/toxrep

Comparative toxicity evaluation of graphene oxide (GO) and zinc oxide (ZnO) nanoparticles on *Drosophila melanogaster*

Kritika Sood[a], Jasreen Kaur[b], Harpreet Singh[a], Shailendra Kumar Arya[a], Madhu Khatri[a,c,*]

[a] Department of Biotechnology Engineering, University Institute of Engineering and Technology, Panjab University, Chandigarh, 160014, India
[b] Center for Nanoscience and Nanotechnology, Panjab University, Chandigarh, 160014, India
[c] Wellcome trust/DBT India Alliance Early Career Fellow, India

ARTICLE INFO

Keywords:
Drosophila
Graphene oxide
Zinc oxide
Nanotoxicity
Nanoparticles

ABSTRACT

Engineered nanomaterials consisting of multiple nanoparticles (NPs) are finding their use in fields as wide and diverse as medicine, environment, cosmetics, energy and electronics. However, health and environmental impacts of these NPs need to be discerned individually to understand their true toxicity. Due to the promising application of upcoming material like GO-ZnO nanocomposite, the toxicity of ZnO and GO NPs was evaluated and compared individually in our study. This study compares the toxicity of Graphene Oxide (GO) NPs and Zinc Oxide (ZnO) NPs synthesized by Green method and Chemical method on *Drosophila melanogaster*. The GO, Chemical ZnO and Green ZnO NPs were synthesized and characterized using SEM, HR-TEM, FT-IR, UV–vis, EDX, XRD and DLS studies. NPs were comparatively analyzed for their cytotoxic and neurotoxic behaviors using different assays like MTT assay, mortality rate, larval crawling and climbing assay, total protein content analysis for evaluating the toxic potential of each of these NPs at different concentrations of use. Green ZnO were found to be least cytotoxic while Chemical ZnO caused the most cell damage. GO were found to have intermediary cytotoxicity. However, a different trend was observed with neurotoxicity wherein Green ZnO reportedly affected the neuromuscular coordination the most, while GO was found to have the least affect. This study provided insights into the different toxic effects caused by GO and ZnO NPs on *Drosophila* as well as comparative toxic effects of Chemical vs Green ZnO NPs.

1. Introduction

The use of engineered nanomaterials (ENMs) based technologies is rapidly and widely increasing in the consumer based era of cosmetics and pharmaceutical industry. ENMs due to their extensive use and lack of proper disposal guidelines are increasingly becoming a threat to environmental health and safety (EHS). There is an increasing concern relating to different types of nanoparticles (NPs) synergistically affecting the EHS upon release into the environment. Many studies have been done to investigate the role of mixed NP exposure on different organisms [1,2]. Tsugita et al. reported a synergistic macrophagic inflammatory response of SiO_2 and TiO_2 NPs [3]. ZnO and TiO_2 NPs that are widely used in cosmetic industries have been reported to have masked effect in each other's presence; wherein ZnO NPs reduced the membrane damage caused by TiO_2 on bacterial cells and TiO_2 decreased the inhibitory effect of ZnO on bacterial ATP levels [4]. Similarly, TiO_2 NPs have been reported to reduce the effect of nano-ZnO and Zn^{+2} ions using *Danio rerio* embryos [5]. Another nanocomposite system that has recently gained popularity is the ZnO-Graphene oxide (GO) nanocomposite, that is being used widely for its efficient photocatalytic and dye degradation applications due to its superior physicochemical properties and application potential for converting solar energy to chemical energy [6–8]. Studies have reported the utilization of GO-ZnO nanocomposite for photocatalytic degradation of various dyes like basic fuchsin dye [7] and methyl orange under solar irradiation [8]. Reduced GO–ZnO nanocomposites (RGO@ZnO) have also been used for various applications like reusable adsorbent for organic pollutants [9], enhanced photocatalysis using sunlight [10], electrocatalysis and supercapacitor applications [11]. Thus, the risk of exposure of such nanocomposites needs to be evaluated at the level of each nanoparticle individually. Many studies have also reported the combined toxic effects of ZnO-GO nanocomposite system. Ye et al. evaluated the effects of ZnO NPs and GO NPs on three aquatic organisms of different trophic levels wherein the toxicity effects were

* Corresponding author at: Department of Biotechnology Engineering, University Institute of Engineering and Technology, Panjab University, Chandigarh, 160014, India.
E-mail address: madhuk@pu.ac.in (M. Khatri).

https://doi.org/10.1016/j.toxrep.2019.07.009
Received 22 April 2019; Received in revised form 29 June 2019; Accepted 25 July 2019
Available online 30 July 2019

additive to *S. obliquus* and *D. magna* but antagonistic to *D. rerio* revealing that toxicity was species dependent. [12]. GO was reported to reduce the bioavailability and toxicity of nano-ZnO in cell viability, oxidative stress, mitochondrial depolarization, and membrane damage in human cell line A549 [13,14].

Although considered as safe by US FDA and listed as GRAS (Generally Recognised As Safe) product, nano- ZnO has been reported to have toxic effects on different organisms using different exposure routes. The most common route of exposure being through skin or inhalation due to its use in cosmetics, pharmaceuticals and IT industries [15]. Many studies have reported ZnO NPs toxicity in mice digestive tract in which primary organs were damaged and the pathological changes induced were both size and dose-dependent [16]. The main toxicity mechanisms of ZnO NPs is the dissolvation of ZnO into free Zn^{+2} ionic form which can cause mitochondrial damage and disruption of cellular homeostasis leading to cell damage [17]. Internalization of ZnO NPs leading to ROS generation upon interaction with cellular membrane and development of oxidative stress upon oral dosage has been reported as main toxicity mechanisms which causes brain damage in rat and mice models [18,19]. Moreover, physical damage due to direct interaction with cells has also been reported to cause cellular toxicity [20]. In case of GO, oxidative stress as well as interaction of GO with cells has been reported to led to increasing levels of reactive oxygen species (ROS) generation thereby causing macromolecular damage like DNA fragmentation, protein denaturation, breakdown of cell membrane lipid, etc. which in turn affects cell signaling and metabolic pathways [21–25]. In the real world scenario, where the risk of exposure of these NPs being released into the environment concurrently is quite high, the toxicity of these nanocomposite materials needs to be assessed individually rather than synergistically for a clearer risk discernment of these nanocomposite systems.

Safety evaluation of ENMs is a necessary step towards realizing their scope in designing different nano biostructures and industrial uses thereby ensuring environment and human safety (EHS). *Drosophila melanogaster* was used as our model organism as offers many advantages like fast offspring turnover, high fecundity, low maintenance cost compared to other model organisms, no strict ethical guidelines for use and high throughput screening methods for detecting induced or abnormal phenotypes [26–28]. The toxicity can be assessed in all stages of development namely- embryonic, larval, pupal, and adult developmental stages and its response to NPs has been shown to be similar to that observed in mammalian models allowing to directly assess the impact of nanoparticle toxicity on the behavior or development. This study was aimed to provide insights into the different toxic effects caused by GO and ZnO NPs individually on *Drosophila* as well as comparative toxic effects of Chemical vs Green ZnO NPs.

2. Materials and methods

2.1. Synthesis of nanoparticles

2.1.1. Synthesis of graphene oxide nanoparticles

2.1.1.1. Chemicals and reagents. Graphite Flakes (99%, Sigma-Aldrich), Sodium nitrate (98%), Potassium permanganate (99%), Hydrogen peroxide (30% wt), Sulphuric acid (98%), Orthophosphoric acid (35%) were all obtained from Himedia. The synthesis of Graphene Oxide nanoparticles were done according to the method described in Marcano et al. [29].

2.1.1.2. Method. Briefly, a 9:1 mixture of concentrated H_2SO_4/H_3PO_4 (108:12 mL) was added to a mixture of graphite flakes (5.0 g, 1 wt equivalent) and KMnO4 (30.0 g, 6 wt equivalent), producing a slight exotherm to 35–40 °C. The reaction was then heated to 50 °C and stirred for 12 h. The reaction was cooled to room temperature and poured onto ice (400 mL) with 30% H_2O_2 (15 mL). The mixture was then filtered through polyester mesh and then centrifuged at 9000 rpm and washed 2–3 times with double distilled water and ethanol alternately. The solid was dried overnight at 60 °C overnight to obtain GO NPs.

The advantages of this method include its simpler and less time consuming procedure, no toxic gas evolution during preparation, and therefore safer to carry out in lab atmosphere for its large scale production [30].

2.1.2. Synthesis of zinc oxide nanoparticles

2.1.2.1. Reagents. Zinc acetate dehydrate (99% pure, Himedia), sodium hydroxide (NaOH pellets, Himedia), fresh leaves of *Corriandrum sativum*, double distilled water (dd-H_2O), Whatman filter paper No 1. The synthesis of ZnO by Green and Chemical methods was done according to Gnanasangeetha et al. [31].

2.1.2.2. Synthesis of zinc oxide nanoparticles by Green method. 50 ml 0.02 M Zinc acetate dihydrate solution was diluted with 50 ml of dd-H_2O and constantly stirred for 10–15 min. Next, 2 ml of aqueous leaf extract of *Corriandrum sativum* were added into the above solution and stirred continuously for about 1 h. To this mixture, 2.0 M NaOH was added to make pH 12 resulting in a pale greenish aqueous solution. This was then placed in a magnetic stirrer for 2 h and later on filtered with Whatman filter paper no. 1 into a glass bottle. The pale green precipitate was then washed with distilled water followed by ethanol in alternate 3–4 times to get rid of any impurities by centrifugation at 9000 rpm for 20 min. A pale greenish white powder of ZnO NPs was obtained after drying at 60 °C in vacuum oven over night.

2.1.2.3. Synthesis of zinc oxide nanoparticles by Chemical method. 50 ml 0.02 M aqueous Zinc acetate dihydrate solution was dissolved in 50 ml dd-H_2O under vigorous stirring for 10–15 min. At room temperature, aqueous 2.0 M NaOH was added drop by drop to reach pH 12 and the resultant solution was then placed in a magnetic stirrer for 2 h and filtered with Whatman filter paper no.1. The white precipitate formed was washed thoroughly with distilled water followed by ethanol to remove the impurities. The precipitate was dried in a hot air oven for overnight at 60 °C. Complete conversion of $Zn(OH)_2$ into ZnO NPs took place during drying.

2.2. Characterization of nanoparticles

Assessing the toxicology of nanoparticles is a challenging task as different particle may have different physico-chemical properties that lead to different biological effects. The characterization was done at Sophisticated Analytical Instrumentation Facility (SAIF), Panjab University, Chandigarh and Central Instrumentation Laboratories, NIPER Mohali. Therefore, the following characterization techniques were employed to nanoparticles:

2.2.1. UV–vis absorbance

UV-Vis analysis was done using the UV–vis-NIR Spectrophotometer Model Lambda 750 (Perkin Elmer). The nanoparticles were analyzed by dispersing in ethanol and sonicating for 5 min before analysis.

2.2.2. XRD analysis

The machine X-ray Diffractometer (Powder Method) Panalytical.s X.Pert Pro was used for XRD analysis of dried powdered samples. The sample patterns were recorded from 10° to 80° using Cu Kα (λ = 1.542 Å) with an accelerating voltage of 40 KV.

2.2.3. FT-IR analysis

Fourier transform infrared spectroscopy (FT-IR) was conducted using F.T. Infra-Red Spectrophotometer Model RZX (Perkin Elmer) to obtain an infrared spectrum of transmission of the nanoparticles. The nanoparticles were analyzed in dried powdered form.

2.2.4. SEM

Scanning Transmission Electron Microscope (SEM) Model JSM6100 (Jeol) with Image Analyser was used for analyzing structure of NPs. The samples of nanoparticles were analyzed in dried form on Cu grid coated with Carbon to increase the conductivity of the sample.

2.2.5. HR-TEM

High Resolution TEM (HR-TEM) was performed using the FEI Tecnai TF 20 UT microscope operated at 200 kV. The nanoparticles were sonicated for 3 min each before analyzing the nanoparticles. Samples were prepared by dispersing the sample in ethanol and depositing it on a hollow Copper grid coated with Carbon to increase conductivity.

2.2.6. EDX

Energy Dispersive X-ray Analysis was done using the FEI Tecnai TF 20 UT microscope operated at 200 kV to reveal the spectra showing peaks corresponding to the elements making up the true composition of the sample. The NPs were sonicated for 3 min before analysis and then dispersed in ethanol and deposited on a hollow Cu grid coated with Carbon.

2.2.7. DLS and Zeta Sizer

Particle size and zeta potential of the powdered NPs was measured by Malvern particle size analyzer (Model: Nano ZS), UK. All the nanoparticles were dispersed in 1:1 ratio of ethanol: water and were sonicated for 5 min before analysis.

2.2.8. Icp-ms

Inductively Coupled Plasma Mass Spectrometry (ICP-MS) was carried out for both types of ZnO NPs and GO NPs at 300 μg/ml concentration in aqueous medium to find out the concentration of ions formed to determine its cytotoxic ability.

2.3. Experimental design

The three nanoparticles (GO, G-ZnO, C-ZnO) were prepared in different dispersions of 1, 10, 50, 100, 200 and 300 μg/ml and were overlaid on surface of fly food in test culture tubes to conduct different experiments as explained below. All experiments were conducted at 25 °C.

2.3.1. Preparation of nanoparticles dispersions

The nanoparticle dispersions were prepared by sonicating the given nanoparticles (GO, G-ZnO, C-ZnO) in double distilled water for 5 min (50 KJ/min) to prepare a stock solution of 1 mg/ml for each of these nanoparticles. Different concentrations of these stock NP dispersions were added to double distilled water to make the final concentrations of 1, 10, 50, 100, 200 and 300 μg/mL (working solutions) that were further used for dosing of flies.

2.3.2. Culturing of flies

The flies of strain Oregon-R that were used for this experimental work were received as a gift from Dr. Lolitika Mandal, IISER- Mohali. The fly food was optimized after certain trials to best fit the optimum growth and nutrition of the flies and it consisted of maize powder, sugar, yeast, agar, nipagin and propionic acid. The flies were transferred to new bottles periodically and the stocks were maintained at 25 °C.

2.3.3. Nanoparticle dosing and controls

In all the experiments, 1 ml of different NP dispersions were used for dosing by overlaying it on the surface of solidified fly food. These test culture tubes were then allowed to dry for 1–2 days before adding flies to it. 2 males and 3 females were added to each vial by anaesthetizing flies using CO_2 exposure and separating under a stereomicroscope. The flies which were exposed to normal fly food (without NPs) were marked as Control and are referred to as 'Untreated Flies' throughout the experiments. All the experiments were performed in triplicates.

2.3.4. Rate of growth and development from egg to adult fly

The rate of development from freshly laid eggs, fed with different concentration of different NPs were studied based on the duration of post embryonic development. For assessing the duration of post – embryonic development, 2 males and 3 females were added to each test vial with different NP type and concentration. The freshly laid eggs were then analyzed and observed for their growth and developmental process based on the incubation period to reach different larval stages and adult longevity of *D. melanogaster* after treatment. The experiment was done in triplicates and comparisons were made with untreated or control flies.

2.3.5. Mortality rate

Mortality rates (MR) were measured according to Prevost et al. on groups of 5 flies/concentration of each type of nanoparticle of *Drosophila melanogaster* [32]. The experiment was performed in triplicates along with the untreated or control flies. Female adult flies (~3 days old) were added to test culture tubes overlaid with different concentration of each type of NPs on food surface and were allowed to complete their development under the optimum conditions of light and temperature (25 °C) over a period of 18 days. The mortality rate was estimated for each type of NP as follows:

$$\mathrm{MR}\% = \frac{\text{Number of dead flies}}{\text{Initial number oflies}} \times 100$$

2.3.6. Crawling assay

Larval crawling ability has been widely used as a reliable parameter for analyzing any early stage changes in the crawling abilities of *Drosophila* larvae and also for determining the effect of drugs or particulate matter like NPs on their locomotion. The larval crawling assay becomes more vital if the expression or abolition of a gene causes mortality in pupal or adult stages and these flies may not survive to adulthood where they otherwise could have been assessed [33].

Third instar larvae (10 per concentration/ nanoparticle) were obtained and put in 5% sucrose solution [33] along with 500 μl of each nanoparticle at different concentration and were allowed to feed for at least 45 min. Next, the flies were graded for their crawling ability using a petriplate in which graph paper was attached to the base and 2% agar was poured over it and allowed to harden. The number of 0.1 × 0.1 squares traversed by each larva per concentration per nanoparticle was recorded for 1 min interval each. The total distance travelled was then calculated and results were recorded graphically [34].

2.3.7. MTT assay

Cellular viability was measured using 3-(4, 5-dimethylthiazol- 2-yl)-2,5 -diphenyltetrazolium bromide (MTT) reduction assay by preparing single cell suspensions (SCC) of *Drosophila* adult flies. Flies were taken from each concentration of the given three nanoparticles after anaesthetizing with CO_2 exposure and a SCC of these flies was prepared after treatment with trypsin containing 1 mM EDTA and mixture of enzymes (collagenase, proteinase K and hyaluronidase) in sterile PBS [35]. The MTT assay was performed in triplicates for determining cell viability by using MTT assay kit (Sigma Aldrich).

The steps were performed according to the protocol described in the kit using different NP exposed *Drosophila* SCC as test samples. Different concentrations of exposed *Drosophila* single cell suspension (Untreated, 10, 100, 300 μg/ml) and that of untreated flies were added in different wells in a 96 well titre plate in triplicates and the plate was incubated at 37 °C, 5% CO_2 for 1 h. MTT reagent was added for a concentration of 10% of the total volume. The plate was returned to the incubator and incubated for 2 more hours. Next, 100 μl of solubilisation buffer was

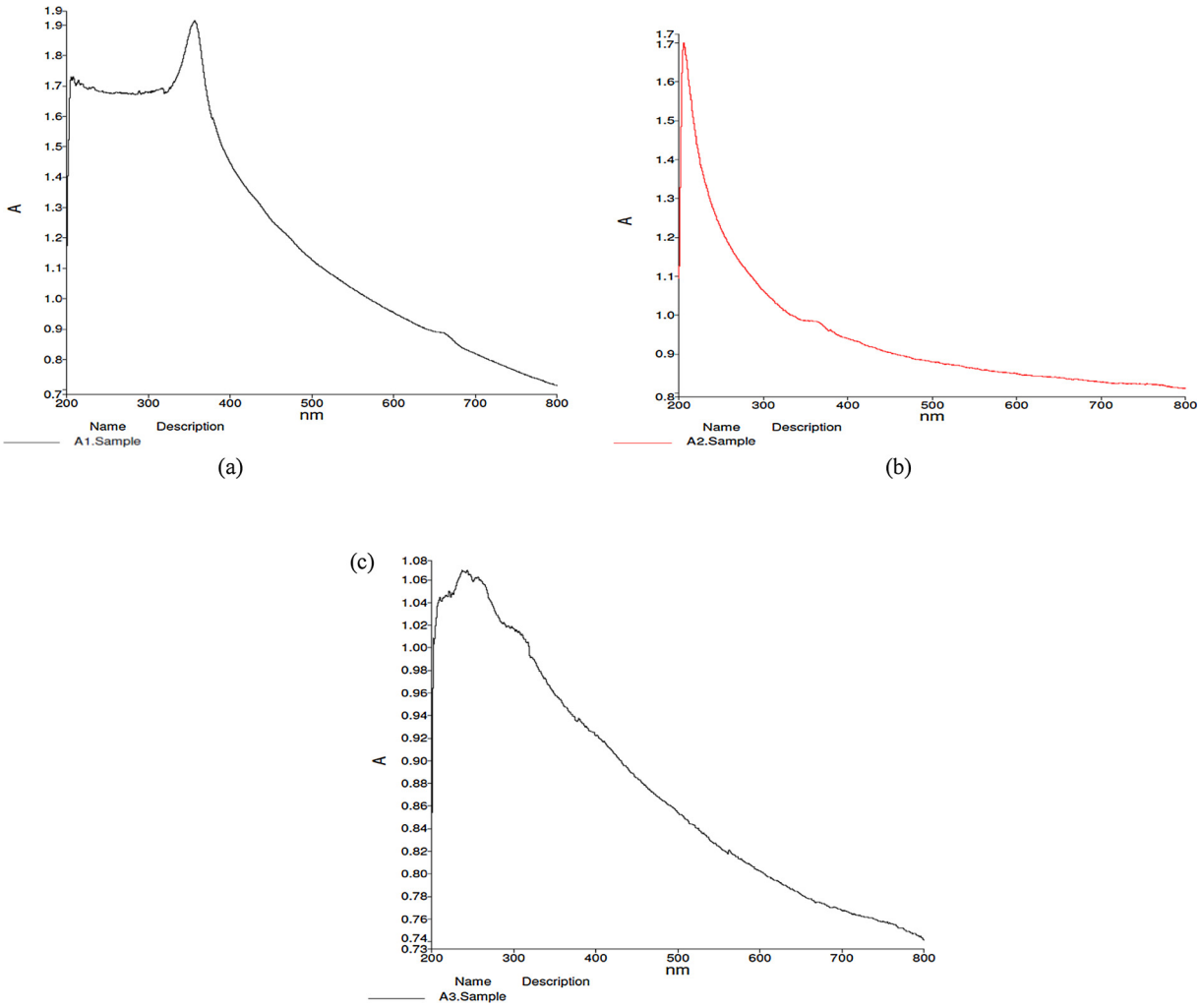

Fig. 1. (a) UV–vis absorbance of G-ZnO (A1). (b) UV–vis absorbance of C-ZnO (A2). (c) UV–vis absorbance of GO (A3).

added to each well of the titre plate and mixed by pipetting up and down repeatedly to dissolve formazon crystals formed. The plate was read at 570 nm in multimode plate reader.

The percent survival of these cells was calculated by using the formula-

$$\text{Viability\%} = \frac{\text{Absorbance of test sample}}{\text{Absorbance of control}} \times 100$$

2.3.8. Climbing assay

The distance at which a third instar larva pupates from its foraging substrate is called the pupation distance. It is a measure of pupation behavior most assays have in common. Early studies of larval pupation behavior used a pupation height assay to measure the distance at which *D. melanogaster* larvae pupated from food in vials as well as to test the fitness/ climbing ability of larvae [36]. Many factors such as presence of moisture, texture and chemical properties of the substrate influence the site of larval pupation [36,37]. Pupation behavior is a polygenically inherited trait wherein the changes can be attributed to either having a small number of major genes with many minor modifiers to those with many genes, each having small additive effects [38].

3 females and 2 males in test vials were exposed to each type of NP at different concentrations and incubated at 25 °C for optimum growth and development. After about 4 days, the growth of third instar larvae of F1 generation was tracked. The pupation distance of third instar larvae that succeeded in pupation was measured at each concentration for each type of NP dispersion. The data was plotted and compared with control (untreated flies). The experiment was repeated three times for each set of NP dispersions and the results were depicted graphically.

2.3.9. Total protein content

To understand the relation between toxicity of different NPs at different concentrations and amount of protein in treated flies, a total protein content analysis of the flies was carried out. Estimation of protein content in untreated as well as NP exposed flies was done according to Bradford method using bovine serum albumin (BSA) as a standard [39].

2.3.9.1. Sample preparation. The larvae (10 flies/experiment; 5 replicates/group) were homogenized in 1 ml of cold homogenizing buffer (0.1 M Phosphate buffer containing 0.15 M KCl; pH 7.4). The supernatant after centrifugation at 9000 *g* was used for estimating total protein content of the samples [40].

2.3.9.2. Preparation of protein reagent. Coomassie Brilliant Blue G-250 (100 mg) was dissolved in 50 ml 95% ethanol. To this solution 100 ml 85% (w/v) phosphoric acid was added. The resulting solution was diluted to a final volume of 1 L. Final concentrations in the reagent were 0.01% (w/v) Coomassie Brilliant Blue G-250, 4.7% (w/v) ethanol, and 8.5% (w/v) phosphoric acid.

2.3.10. Statistical analysis

All the experiments were done in triplicates and were repeated

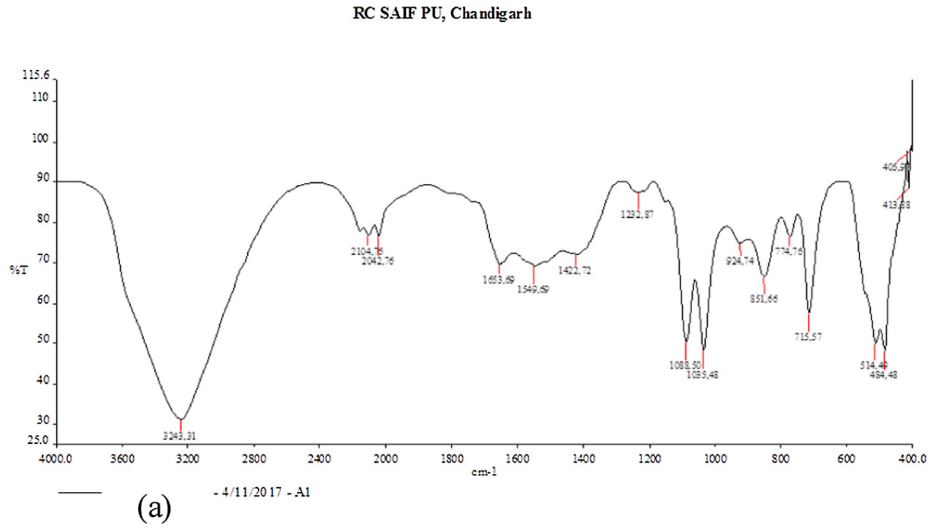

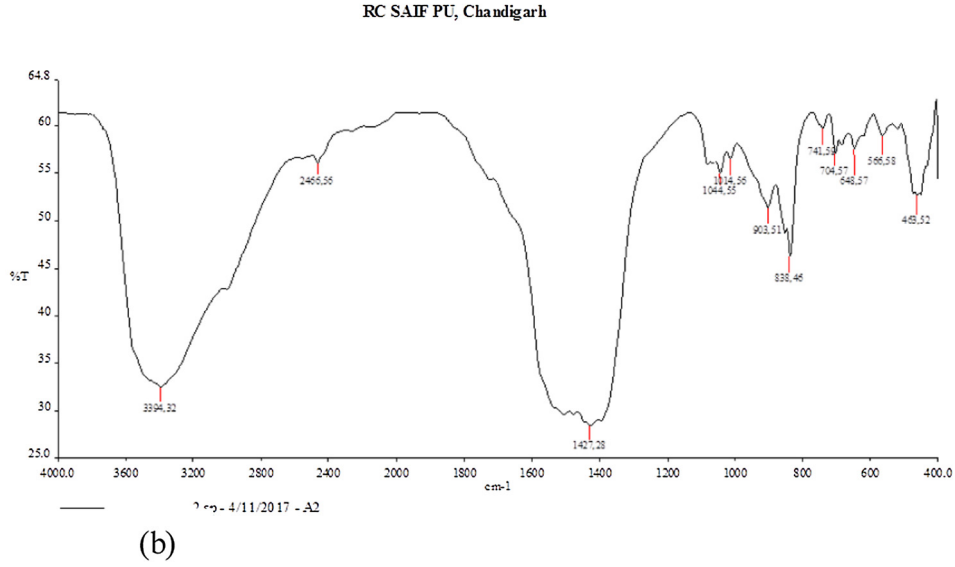

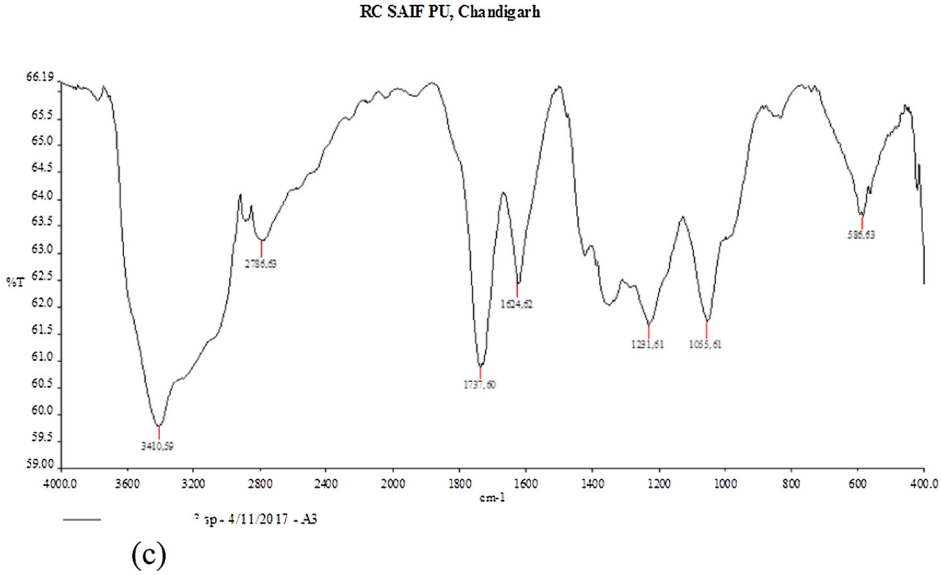

Fig. 2. (a) FT-IR results of Green ZnO (G-ZnO; sample code A1). (b) FT-IR results of chemical ZnO (C-ZnO; sample code A2). (c) FT-IR results of graphene oxide (GO; sample code A3).

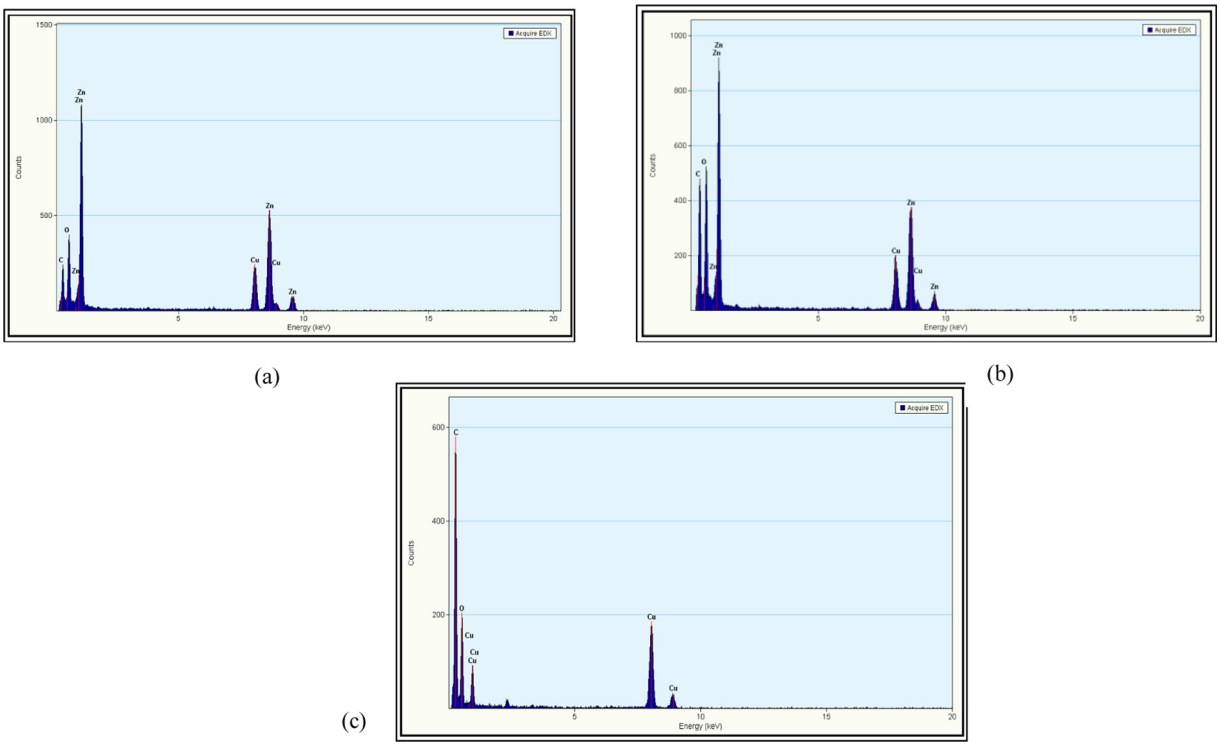

Fig. 3. EDX results of Green ZnO (G-ZnO). (b) EDX results of chemical ZnO (C-ZnO). (c) EDX results of graphene oxide (GO).

twice. Mean values and standard deviations were calculated for all observations and the graphs were plotted. Statistical analysis was performed using Student's *t*-test and One way ANOVA (at $\alpha = 0.05$) with the control values to determine the significant values by using MS-Excel 2016. The values with $p < 0.05$ (*) and $p < 0.01$ (**) were considered to be statistically significant.

3. Results

3.1. Characterization of nanoparticles

3.1.1. UV–vis absorbance studies

The absorption spectrum of both green and chemically synthesized ZnO NPs is shown in Fig. 1(a) and (b) respectively. G-ZnO (A1) exhibits a maximum absorbance at about 357 nm while C-ZnO (A2) exhibits maximum absorbance at 206 nm depending upon the method of synthesis. The absorbance is within UV range and in agreement with the previous studies [41,42]. The sharpness in the peak of absorption of chemically synthesized ZnO NPs indicates the monodispersed nature of the nanoparticle distribution. The absorption maxima obtained for GO (A3) at 237 nm as shown in Fig. 1(c) is in accordance with the previous studies [43,44]. A shoulder peak at ˜300 nm is obtained suggesting n→π* transition of carbonyl group. The maximum absorption (λ_{max}) value indicates the degree of retention of conjugation in carbon rings in the basal planes. This is due to the fact that the more are the number of π→π* transitions (conjugation), the lesser is the energy used for the electronic transition therefore resulting in a high λ_{max} value [29].

3.1.2. FT-IR analysis

Fig. 2(a) depicts the FT-IR spectra of Green ZnO NPs. The pattern of absorption at 715 cm^{-1} and 774 cm^{-1}, 851 cm^{-1} aromatic C–H out of plane bending is a typical mono substituted benzene ring 1,2,3 trisubstituted benzene ring and 1,4 di-substituted benzene ring. The band at 1035 cm^{-1} corresponds to C–N stretching vibration of amine. Medium absorption in the region 1653–1422 cm^{-1} (at 1653 cm^{-1}, 1549 cm^{-1}, 1422 cm^{-1}) often implies an aromatic ring. Two weak IR absorption peaks at 2042 cm^{-1} and 2104 cm^{-1} correspond to C≡C stretching vibration. The broad and intense band at 3243 cm^{-1} depicts the −OH (hydroxyl bond) stretching. Absorption in the region between 405-514 cm^{-1} identifies the presence of ZnO NPs. Absorption IR bands at 1232, 1088 cm^{-1} show the presence of ester group (R—O—R) and C–O bond stretching vibrations and IR peak at 924 cm^{-1} correspond to C═C bond of aromatic compounds present as phytoconstituents in plant extract that remained bound to surface of NPs possibly to enhance the stabilization of ZnO NPs by covering them in the aqueous medium [31]. This shows that the phytoconstituents resisted inspite of repeated washings. Present in the form of aldehydes, amines, terpenoids and phenolic/aromatic compounds were still bound to the surface of ZnO NPs.

Fig. 2(b) depicts the FT-IR spectra of Chemical ZnO NPs. The broad and intense absorption band at 3394 cm-1 corresponds to hydrogen bonded O—H stretching vibration. The absorption band at 2466 cm^{-1} is due to asymmetric C_{sp3}-H bond of the alkyl group. The weak IR peaks between 1000-670 cm^{-1} are due to out of plane C–H bond bending vibrations. The absorption band at 1427 cm^{-1} and 1044 cm^{-1} correspond to ester bond (R—O—R) or C–O bond stretching vibration. The region between 566- 463 cm^{-1} confirms the presence of ZnO NPs in the sample.

Fig. 2(c) depicting the FT-IR spectra of GO NPs revealed the following functional groups: O—H stretching vibrations at 3410 cm^{-1}, C═O stretching vibrations corresponding to peaks at 1720-1737 cm^{-1}, C═C from unoxidized sp^2 CC bonds (1590–1624 cm^{-1}), and symmetric stretch of C–O vibrations at 1250 cm^{-1} in accordance with Marcano et al. [29]. The absorption peak at 586 cm^{-1} corresponds to C—H deformation vibrations. The peak at 1624 cm^{-1} correspond to C═C stretching vibrations of graphene, C—O alkoxy bond vibrations at 1055 cm^{-1} and the absorption at 2700–2900 cm^{-1}can be attributed to deforming vibration of C—H bond [45].

3.1.3. EDX results

According to Fig. 3(a) and (b), the EDX spectra of G-ZnO and C-ZnO are similar in elemental composition. Only elements Zn and O prove

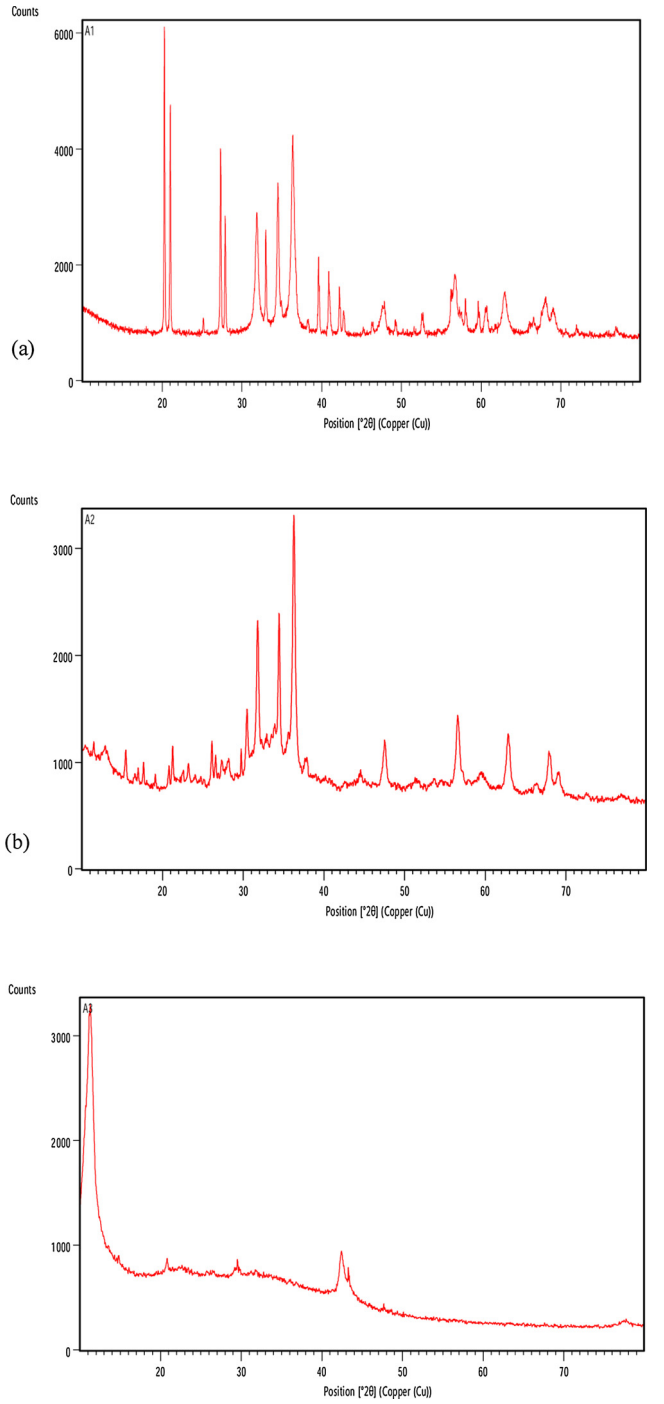

Fig. 4. (a) XRD pattern of Green ZnO (G-ZnO; sample code A1). (b) XRD pattern of chemical ZnO (C-ZnO; sample code A2). (c) XRD pattern of graphene oxide (GO; sample code A3).

that the NPs synthesized are pure and no other elemental impurities were reported. The peaks of Cu and C are due to the grid material used for analyzing the sample. The grids used were that of Cu and were coated with Carbon to increase conductivity of non-conductive samples.

Fig. 3(c) represents the EDX spectra of GO. The high peak intensity of Carbon can be attributed to both the sample C (in form of Graphene Oxide) as well as C coating on the sample. Other elements are Oxygen (O) present as a proof of oxidation of graphite to GO NPs. Other small peaks that are present and not labeled may correspond to fact that the element has already been labeled or that the element does not exist in a significant amount to be taken in account.

3.1.4. XRD analysis

The XRD pattern of nanoparticles synthesized by Green method and Chemical method shown in Fig. 4(a) and (b) respectively were recorded on an X-ray diffractometer using Cu (kα) radiation (λ = 1.5415 Å) operating at 40 kV and 30 mA with 2θ ranging from 10°-80°. Distinctive peaks of Green ZnO at 2θ values were 20.25, 20.98, 27.28, 27.87, 31.81, 32.94 34.47, 36.32, 56.67, 60.61, 62.95, 68.10, 69.04. The highest peak was observed at 2θ value 20.25 with d-spacing value of 4.37 Å. X-ray diffraction of Chemical ZnO NPs synthesized show 2θ values at 30.48, 31.75, 34.45, 36.28, 56.58, 59.50, 62.85, and 67.97. The highest peak was observed at 2θ value 36.28 with d-spacing value of 2.47 Å. High purity and crystallinity of the prepared ZnO NPs were confirmed by sturdy and clear peaks. For other impurities no characteristic peak was accessible [46]. The increase in the d-spacing (4.37 Å) of Green ZnO which causes a shifting of peak corresponding to a lower 2θ value (20.25) than Chemical ZnO is due to tensile stress indicating distortion of structural planes [47]·

The X-ray diffractograms of the GO samples shown in Fig. 4(c) exhibited a distinct diffraction peak at around 11° and another at about 42-43° in accordance to Marcano et al. [29]. A very small peak located at around $2\theta = 21^{\circ}$, suggested small changes in the crystal structure of GO corresponding to d spacing of 3.380 Å which might be attributed to very thin RGO layers due to high degree of exfoliation.

Graphite usually exhibits basal reflection peak between 2θ = 24–26 degree with corresponding d values of 3.34 − 3.36 Å. Upon oxidation of graphite, the reflection peak as shown in Fig. 4(c) can be seen shifted to the lower angle (at 2θ = 11.31° and d spacing = 7.81 Å) which is in accordance to results obtained by Marcano et al. [29] indicating oxidation of graphite. The increase in d-spacing is due to the intercalation of water molecules and the formation of oxygen containing functional groups between the layers of the graphite.

3.1.5. HR-TEM/SEM image analysis

3.1.5.1. Green zinc oxide nanoparticles. Fig. 5(a) HR-TEM image of Green ZnO NPs at 5000× magnification while (b) shows the HR-TEM image at 19000X magnification. The images show that both conical/irregular shaped as well as spherical nanoparticles are formed and some can be seen in clusters depicting aggregation of these nanoparticles. (c) SEM image of Green ZnO at 1000× magnification while (d) shows the SEM image at 3000X magnification. Profiles (a) and (b) clearly show that the size of these NPs range from 450 to 500 nm.

3.1.5.2. Chemical zinc oxide nanoparticles. Fig. 6(a) HR-TEM image of Chemical ZnO NPs at 5000× magnification while (b) shows the HR-TEM image at 19000× magnification. Both rod shaped as well as flower shaped nanoparticles were formed and some of these can be seen in clusters. HR-TEM image profiles Fig. 6(c) and (d) at 29,000× and 19,000× magnification clearly depict that the product obtained is in flower form which is in close agreement to Gnanasangeetha et al. [31].

3.1.5.3. Graphene oxide nanoparticles. In order to probe the morphology of GO, HR-TEM was performed. Ethanol dispersion of graphene oxide was used for HR-TEM after sonicating the sample for 3 min. Fig. 7(a) HR-TEM image of GO NPs at 5000× magnification while (b) shows the HR-TEM image at 19,000× magnification. Bends and wrinkles on GO nanosheets at several places as can be seen in Fig. 7 profiles (b) and (c) may have been originated by various defects and functional groups carrying sp^3 hybridized carbon atoms, which are introduced during the oxidation process. Fig. 7(c) HR-TEM image of GO NPs at 29,000× magnification while (d) shows the SEM image at 500× magnification. (e) HR-TEM image at 240,000× magnification clearly depicting the GO nanosheets formed. In general, GO nanosheets tended to assemble with each other and forms multilayer agglomerate.

3.1.6. DLS and zeta potential results

The DLS and Zeta Potential results are summarized in Table 1. The

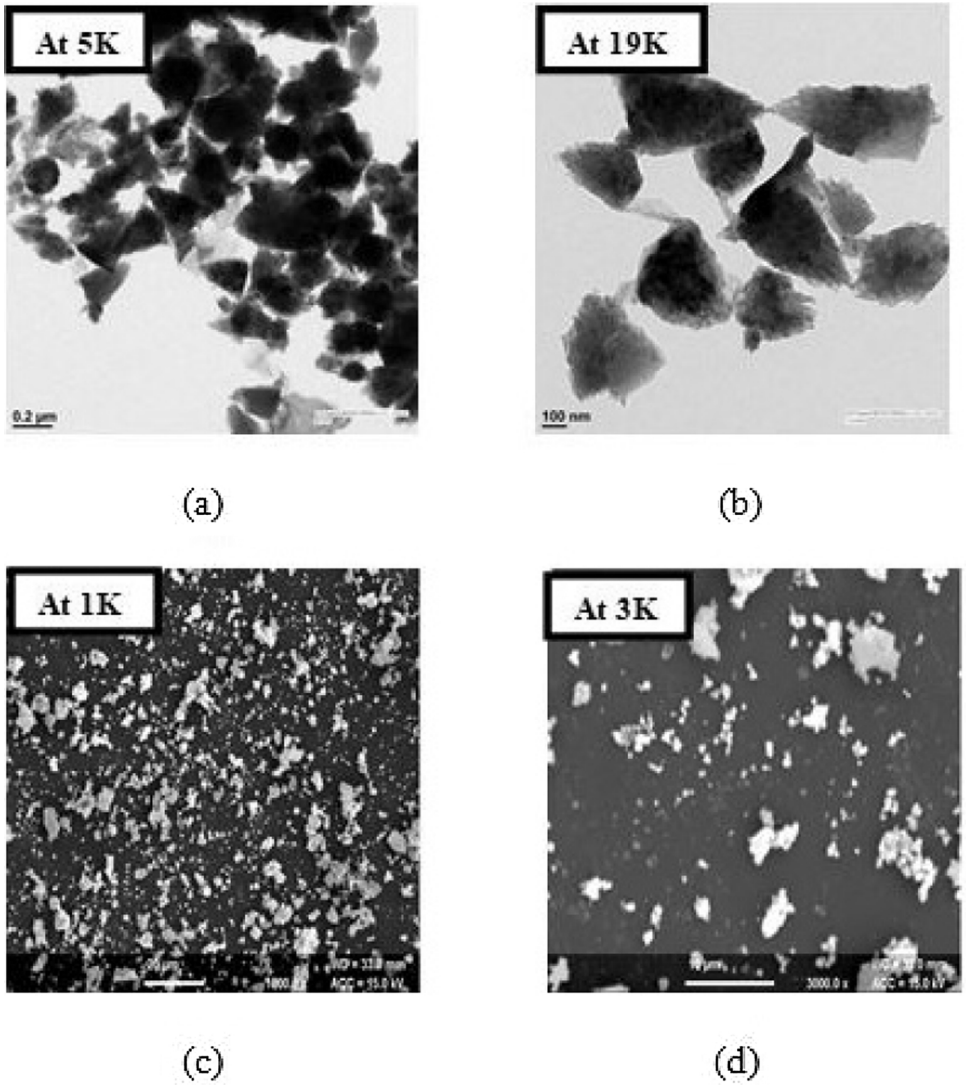

Fig. 5. (a) HR-TEM image of Green ZnO NPs at 5000× magnification. (b) HR-TEM image of Green ZnO NPs at 19,000× magnification. (c) SEM image of Green ZnO at 1000× magnification. (d) SEM image of Green ZnO at 3000× magnification.

DLS results show the average size of green ZnO NPs ˜ 498 nm while that of chemical ZnO and GO NPs is 519 nm and 780 nm respectively. The zeta potential of green ZnO (− 33.5), chemical ZnO (-26.93) and GO (-31.06) which are all more than -25, indicating high degree of stability of these NPs in solution and lesser chances of aggregation. The polydispersity index (PdI) of green nanoparticles is 0.249, chemical ZnO NPs is 0.409 and GO is 0.469 which are all less than 1, showing less aggregation of nanoparticles, which is a good sign signifying that the most of the nanoparticles in the sample are monodispersed.

3.1.7. ICP-MS analysis

ICP-MS analysis revealed that the concentration of ions formed by ZnO and GO NPs were less than 10% in each case and thus might not have played a significant role in contributing towards the toxicity caused by these NPs as reported elsewhere [17]. However, in our studies, the role of dissolution of NPs into respective ions is negligible as these NPs were overlaid on solidified food media and not in aqueous solution wherein the NPs would readily be dissociated into its respective ions.

3.2. Effect of nanoparticles on growth rate and development

The effect on the growth and development of the flies was recorded in Table 2 and it was observed that different NPs were affecting the growth differently at 100 μg/ml concentration. A normal/untreated fly completed its course of development in 7–8 days usually while a fly treated with Chemical ZnO NPs took more than normal time i.e. usually about 9–10 days. This in turn affected the total number of flies formed in a fixed period of time. Starting from 5 flies (2 male and 3 females in each set) initially, Chemical ZnO treated group recorded 10 flies in 15 days while the control recorded about 15 flies in 15 days. It was also observed that flies treated with Green ZnO NPs developed quickly until the larval stage but their pupation was usually slower than flies treated with GO NPs. The GO treated flies had slower development until the larval stage as compared to Green ZnO treated flies but the number of flies were almost at par with the untreated group. At the end of 15days, the Green ZnO treated flies were recorded as the highest in number i.e. 21 flies while the Chemical ZnO treated flies were 11 in number which is lower than an average of 15–17 flies in untreated samples. Flies that were exposed to GO were 15 in number, which is at par with the untreated flies.

3.3. Morphological analysis

The morphological analysis of the flies was done in terms of skin color, eye pigmentation and wings that may affect its ability to fly. A

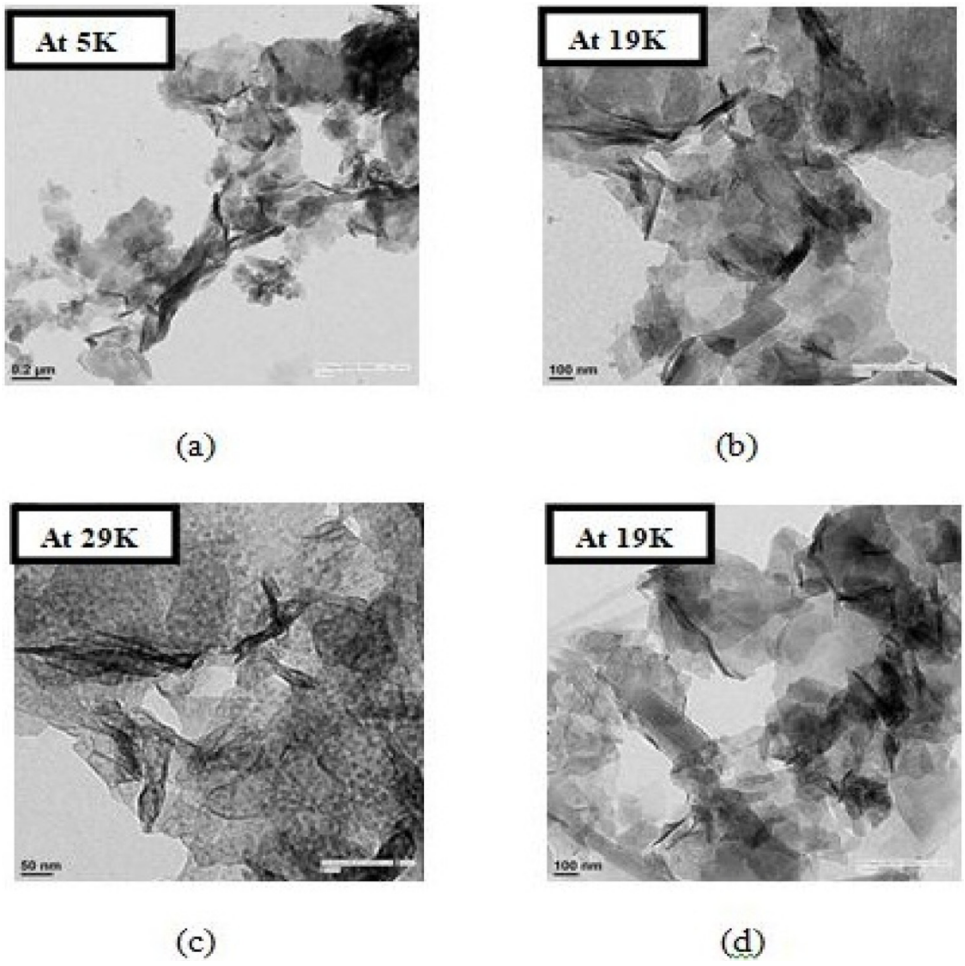

Fig. 6. (a) HR-TEM image of Chemical ZnO NPs at 5000× magnification. (b) HR-TEM image of Chemical ZnO NPs at 19,000× magnification. (c) HR-TEM image profile at 29,000× magnification depict that the product obtained is in flower form. (d) HR-TEM image profile at 19,000× magnification clearly depict that the product obtained is in flower form.

few flies were observed to be unpigmented in 1 µg/ml Chem ZnO and 10 µg/ml and 100 µg/ml Green ZnO. Similar results have been reported by Tyagi et al. [48]. These unpigmented flies had low flight and remained stuck to the food mostly. On the other hand, the control flies were pigmented in all abdominal segments and had no flight defects. As the epidermal pigments are secreted by the cuticle, so a cuticle defect is likely the root cause of these changed phenotypes [48]. No pigmentation change was found in GO treated flies. The eye color was red in all treated as well as untreated flies consistent to the strain (Oregon R).

3.4. Mortality rate

As shown in Fig. 8, the mortality rate percent of flies were recorded and the results revealed that highest concentration of GO NPs (100 µg/ml and 300 µg/ml) caused 100% mortality (all flies dead) within the lowest time 16 days and 14 days respectively. This shows that high concentrations of GO NPs were lethal to the flies and the toxicity effects are concentration dependent. In comparison, all concentration of Chemical ZnO exposed and Green ZnO exposed flies took a minimum of 18 days to reach 100% mortality. Chemical ZnO are more toxic (60% mortality) than Green ZnO NPs (40% mortality) 100 µg/ml concentration after 2 weeks exposure. However, both ZnO NPs exerted almost identical toxicity at a concentration of 10 µg/ml and 300 µg/ml (80% mortality) after 2 week exposure to flies. All NPs caused mortality after about a week of exposure indicating that prolonged exposure was responsible for lethality. The control recorded about 20% mortality on the 12^{th} day and it reached upto 40% by the end of 18 days. Thus, the effect of NPs is directly related to time of exposure in addition to the type of NP and its concentration of exposure. The state of aggregation is greater in higher concentration of NPs, which may sometimes delay the potential toxic effects.

3.5. Larval crawling assay

The results of the larval crawling assay are shown in Fig. 9(a). The exposure of GO nanoparticles to larvae resulted in a non-monotonic trend with the larval crawling decreasing steadily upto a concentration of 50 µg/ml and then increasing up to 200 µg/ml. the number of squares crossed by larvae exposed to 300 µg/ml of GO NPs was the least indicating fatal damage to the neuromuscular coordination of these larvae. This can be confirmed by the mortality test results, which showed these nanoparticles to be the most toxic. However, the trend with increasing concentration of exposure of both green and chemically synthesized nanoparticles is the same i.e. it decreases up to a certain concentration, and upon reaching 100 µg/ml, it gives a notable hike and then decreases again until 300 µg/ml. This indicates that both these nanoparticles affect the larvae in a somewhat similar manner although the average no. of squares crossed by larvae in green ZnO is greater than chemically synthesized ZnO nanoparticles. The concentration of 100 µg/ml is somewhat pivotal and signifies a change in neuronal activity of the larvae thereby affecting its neuromuscular coordination and hence it's crawling ability. Sometimes, the higher state of aggregation at higher concentration of NPs leading to overall increase in the size of these particles might also delay or decrease their potential

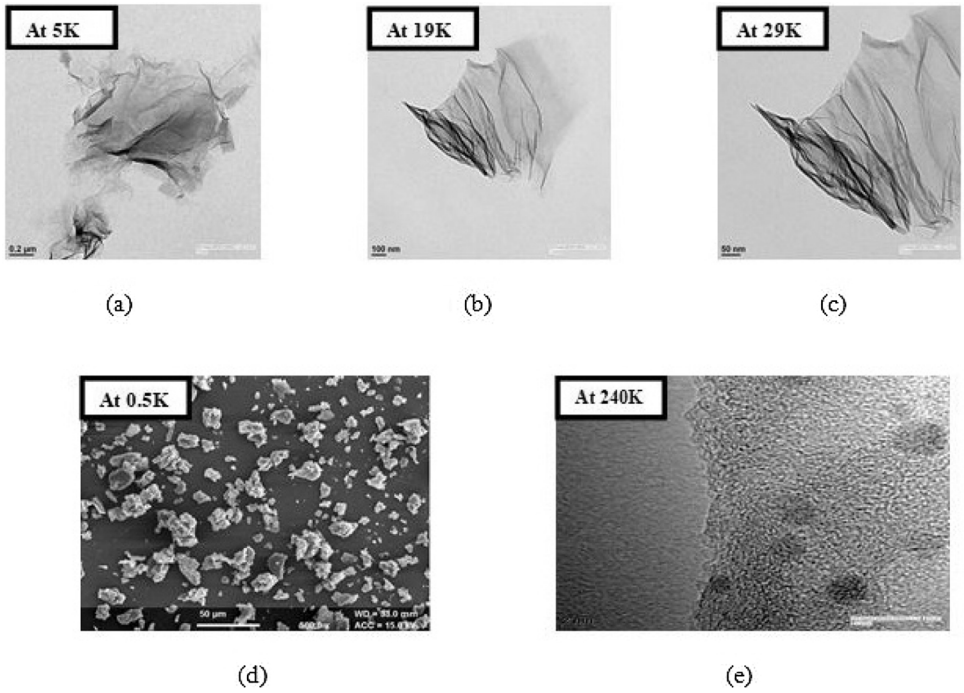

Fig. 7. (a) HR-TEM image of GO NPs at 5000× magnification. (b) HR-TEM image of GO NPs at 19,000× magnification. (c) HR-TEM image of GO NPs at 29,000× magnification. (d) SEM image of GO NPs at 500× magnification. (e) HR-TEM image at 240,000× magnification clearly depicting the GO nanosheets formed.

Table 1
DLS, Zeta potential and pDI results of nanoparticles.

NPs	DLS (nm)	Zeta potential (mV)	PdI
Green ZnO	498.93	−33.5	0.249
Chemical ZnO	519.33	−26.9	0.409
Graphene Oxide	780.11	−31.0	0.469

toxic effects. However, further studies would be needed to quantify and assess the changes observed with such behavior in these larvae.

3.6. Climbing assay

Pupation height is a behavioral trait that has a considerable effect on the fitness of the larvae [38]. Since all the other nutritional components as well as abiotic components were the same, the differences in pupation heights can be attributed to the exposure of different NPs at different concentrations to the larvae of F1 generation. The highest pupation height was recorded in Green ZnO at 100 µg/ml concentration as shown in Fig. 9(b). This indicates that 3rd instar larvae of Green ZnO were engaged in prepupation behaviors such as foraging and locomotion to quite a high extent. This can be confirmed by the crawling assay results in which the third instar larvae crossed the maximum no. of squares when exposed to 100 µg/ml concentration. The average crawling was maximum in case of Green ZnO as was shown in the Fig. 9(a). Since larvae do not feed during the wandering period, prepupation behaviors primarily depend on energy stores acquired during the foraging period of larval development (i.e., during the first, second and half of the third instar). GO NPs at lower concentrations almost mimic the pupation height of the control. However, pupation height in Chemical ZnO is more than that observed in GO NPs. Also, the larval development time plays a significant role in pupation height [49], which confirms the early larval development (Table 2) at 100 µg/ml concentration in Green ZnO NPs than control samples or any other NPs (Chemical ZnO and GO NPs) at the same concentration. (Table 3)

3.7. MTT assay for cell viability

The MTT assay results (Fig. 9 (c)) revealed the percent viability of cells exposed to different NPs at different concentrations. The MTT absorbance recorded is in direct proportion to the living cells as the MTT dye preferentially stains the live cells. The highest viability percent was recorded in Green ZnO while the lowest cell viability was recorded in Chemical ZnO. This confirmed that Green ZnO caused minimum cell damage while Chemical ZnO caused highest cellular damage and is thus the most toxic at cellular level. GO NPs posed intermediate cell damage between that of Green ZnO and Chemical ZnO. Furthermore, the cell damage was concentration dependent and increased with increasing the concentration of NP exposure i.e. cellular toxicity was highest in 300 µg/ml of Chemical ZnO and lowest in 100 µg/ml of Green ZnO while the toxicity posed by GO was observed to be intermediary level. Thus, the significant drop in cell viability at higher concentrations of Chemical ZnO confirmed it to be the most toxic at cellular level.

3.8. Total protein content

The trend of total protein content is rather different with different NPs as shown in Fig. 9(d). The protein content of flies treated with

Table 2
ICP-MS analysis of nanoparticles at 300 µg/ml.

	Green ZnO-[Zn^{+2}] [µg/ml]	Chemical ZnO-[Zn^{+2}] [µg/ml]	[GO]-[µg/ml]
Concentration of ions	21.04 ± 2.12	28.88 ± 2.52	12.26 ± 0.86
Approx. (%)	7.01	9.62	4.08

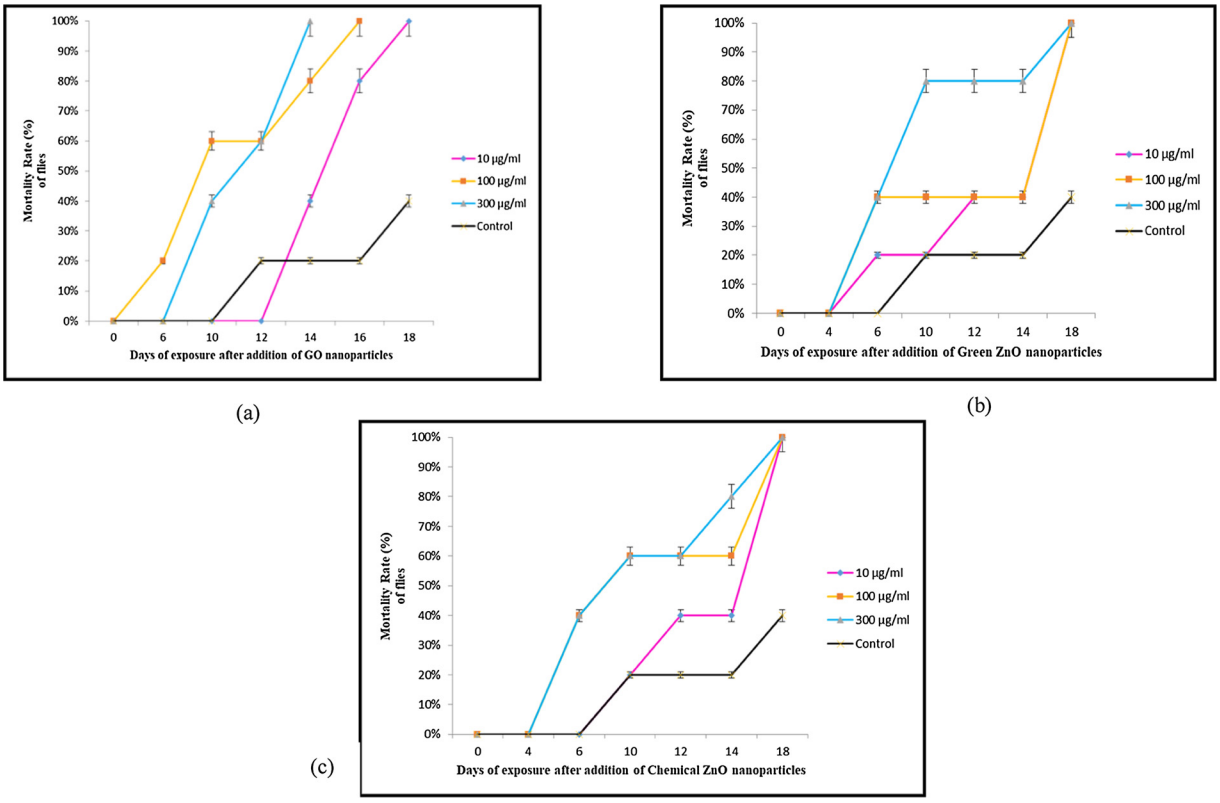

Fig. 8. Mortality rate (%) of flies after exposure of (a) GO NPs (b) Green ZnO NPs and (c) Chem ZnO NPs.

Green ZnO decreases with increasing the concentration of NPs indicating the level of protein expression changed significantly at lower concentration of 10 µg/ml ($p < 0.01 = **$) which may be attributed to the fact that NPs are lesser aggregated at lower concentration and hence cause more cytotoxicity by penetrating inside the cells. In Chemical ZnO, the trend is reversed with total protein content increasing with an increase in NP concentration. This may be due to lesser aggregation and smaller size of NPs wherein 100 µg/ml and 300 µg/ml of Chemical ZnO are significant values ($p < 0.05 = *$). GO NPs show a somewhat similar trend and the total protein content increases with increasing concentration of NPs however, the values are somewhat closer to the control group with a significant value at 100 µg/ml ($p < 0.01 = **$). The results show that the total protein content changes with the type of NPs used at different concentrations confirming that all these NPs are causing cytotoxicity by changing the levels of protein transcribed by some important genes.

4. Discussions

This is one of the few studies that are done to assess both the behavioral as well as cytotoxic effects of real world nanoparticles such as ZnO and GO NPs on *Drosophila melanogaster* to determine their effect individually rather than synergistically in a GO-ZnO nanocomposite system. This study interestingly points out the detrimental effects of both green and chemically synthesized ZnO NPs and GO NPs on the growth and development, crawling and climbing ability of the flies as well as their cytotoxic potential at predefined concentrations, surprisingly highlighting the toxic effects of green nanoparticles. Similar to previous studies [50–52], we observed that the mortality rate as well as the cell viability of the flies were affected in a dose-dependent and time dependent manner.

The unique properties of nanoparticles related to its size, shape, surface area, charge, solubility, surface chemistry and dispersion factor play a key role in determining the cytotoxic potential of nanoparticles [53–55]. Different NPs have different unique properties that play a vital role in deciding their toxicity. The size of nanoparticles plays a vital role in its toxic potential [21]. In our study, GO nanosheets due to their large size and sharp edges could have caused physical damage to the cell membrane leading to the increased permeability of mitochondrial membrane causing stress thereby altering its membrane potential [21,22]. This could have led to decreased cell viability and possible reason for mortality of F0 flies as indicated in cell viability and mortality assay respectively. Oxidative stress could also be one of the main mechanisms involved in toxicity caused by GO causing mortality in flies. The interaction of GO with cells could have led to increasing level of reactive oxygen species (ROS) generation which might have led to macromolecular damage like DNA fragmentation, protein denaturation, breakdown of cell membrane lipid, etc. which in turn affects cell signaling and metabolic pathways [21], [23]. Oxidative stress due to increasing levels of ROS might have reduced the activity of antioxidant enzymes like catalase, SOD, or glutathione peroxidase (GSH-PX) [56]. ROS generation thus, could have been one of the mechanisms through which GO NPs could have posed cytotoxicity to *Drosophila* at different developmental stages of its life cycle. ZnO NPs have been reported to be neurotoxic in mice by increasing the oxidative stress level in the brain [19]. The uptake of ZnO NPs leading to ROS generation upon interaction with cellular membrane and development of oxidative stress upon oral dosage (same in case of flies) could have been the main toxicity mechanisms in this study as reported in previous studies [18,19]. Therefore, somewhat similar mechanism might have led to an imbalance in the neuromuscular coordination of the larvae and hence increased crawling was observed in case of ZnO NPs as observed in larval crawling assay. Moreover, the mechanical and oxidative damage due to their direct interaction with cells could have also led to cytotoxicity [20]. Also, the method of synthesis played a major role towards the cytotoxic potential of ZnO NPs. The Green ZnO NPs due to their “green route” of synthesis utilised phytoconstituents as capping agent, which due to their antioxidant properties posed lesser cytotoxicity than

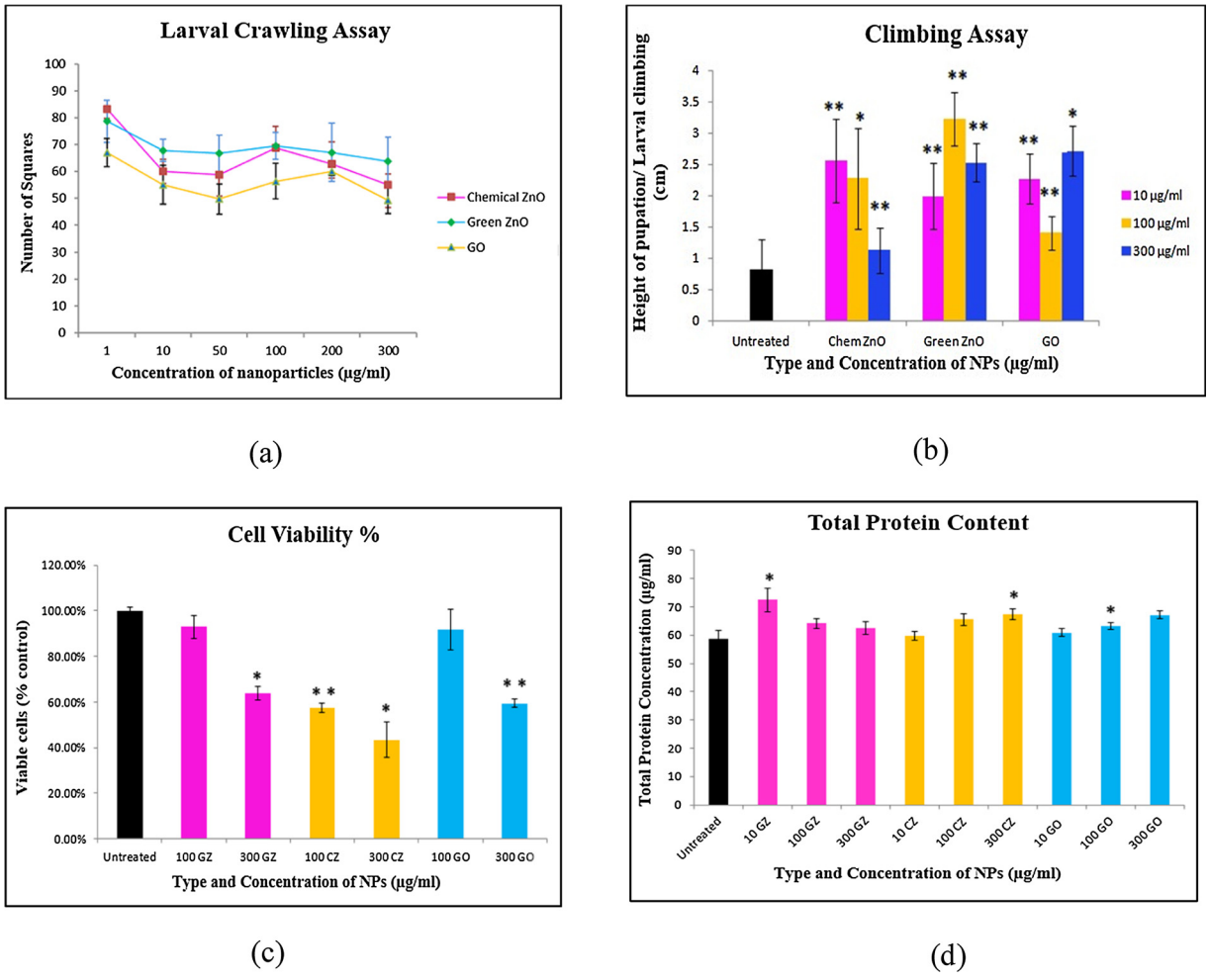

Fig. 9. (a) Crawling assay analysis (Chem ZnO vs Green ZnO vs GO NPs). The average no. of squares crossed by larvae treated with Green ZnO is the greater than the average no. of squares crossed by larvae treated with both Chemical ZnO and GO. (b) Climbing assay indicating the pupation distance for F1 generation recorded for different NP concentrations (*= $p < 0.05$ and **=$p < 0.01$). (c) Relative viabilities (% control) of cells recorded for different NPs at different concentrations. (GZ = Green ZnO, CZ = Chem ZnO, GO = graphene oxide NPs.) (*= $p < 0.05$ and **=$p < 0.01$). (d) Protein content recorded for flies exposed to different NPs (GZ = Green ZnO, CZ = Chem ZnO, GO = graphene oxide NPs) at different concentrations (*= $p < 0.05$ and **=$p < 0.01$).

Table 3
Growth and Development record of flies with different NPs at a concentration of 100 µg/ml.

Type of NPs/ No. of days	Control	Green ZnO(100 µg/ml)	Chemical ZnO(100 µg/ml)	GO NPs (100 µg/ml)
Day 1	Egg hatches	No egg	No egg	No egg
Day 2	1st instar observed	Egg hatches	No egg could be observed	Egg hatches
Day 3	Some 2nd instar were observed along with 1st instar	1st instar along with very few 2nd instar observed	Egg hatches	1st instar observed
Day4	Few 3rd instar larvae could be seen crawling in the food	Few 3rd instar larvae observed	1 dead fly along with 1st and few 2nd instar observed	2nd instar could be observed
Day 5	Pupa formation observed	Many 2nd and 3rd instar larvae could be seen + very few pupa	Very few 3rd instar with many 1st and 2nd instar, 1 pupa also observed	3rd instar larvae could be seen + few pupa observed
Day 6	Pupa entering into adult	Many more new pupae seen	3rd instar larvae and few pupa seen	Many pupae could be seen
Day 7	Ready to emerge from pupa case	Adult	Many more new pupae seen	Ready to emerge from pupa case
Day 8	Adult	–	Pupa developing	Adult
Day 9	–	–	Adult	–

pure Chemical ZnO NPs as evident in cell viability and mortality rate assays. Green ZnO NPs fared the highest in larval crawling assay signifying that the neuromuscular coordination was a bit off in these NPs especially at a concentration of 100 µg/ml wherein the larval crawling was reported to be maximum. Green ZnO NPs also showed signs of early development of larval stages thereby producing greater number of flies than control set indicating that these NPs caused a stimulating effect on the growth and developmental genes of the exposed flies which may be attributed to the plant phytochemicals with antioxidant properties in comparison to chemically synthesized NPs. Chemical ZnO NPs due to its small size and different chemistry than GO NPs posed higher toxicity in cell viability assay and affected the rate of growth and development of flies. The state of aggregation of NPs also determines the toxic potential of nanoparticles in addition to the size of NPs. This could be the case for

Green ZnO which although smaller in average size than Chemical ZnO NPs were found as aggregates in water as confirmed by its HR-TEM and UV–vis absorbance. Hence, state of aggregation could also have been one of the reasons due to which Green ZnO or GO NPs could not have realized their toxic potential and were found to be lesser toxic in most cases than Chemical ZnO. The state of high aggregation in Green ZnO inspite of its lesser size could be attributed to lesser viability of cells in MTT assay and affected the rate of growth and development of flies. Also, the concentration of NPs used during dosage also play a major role in determining the toxic effects of these NPs on *Drosophila*. The negligible dissolvation of ZnO NPs into Zn^{+2} ions might not have caused toxicity as explained earlier. However, all these proposed mechanisms of toxicity need to be explored further which opens up new avenues of research in this field. This study provided insights into the different toxic effects caused by GO and ZnO NPs on *Drosophila* as well as comparative toxic effects of Chemical vs Green ZnO NPs.

5. Conclusions

In summary, NPs used in this study depending upon their differential composition and physiochemical properties resulted in different biological responses in the flies and caused toxicity (either cytotoxic or neurotoxic) at different concentrations upon prolonged exposures and hence should be avoided in articles of daily use like cosmetics, food packaging, pharmaceuticals etc. and if employed elsewhere should be used at lower concentrations and within permissible limits. The high mortality rate of flies and morphological changes observed upon prolonged exposure at high concentrations provides cues towards the use of these nanoparticles in the field of insect and pest management.

Declaration of competing interest

The authors declare that they have no known competing financial interests or personal relationships that could have appeared to influence the work reported in this paper.

The authors declare the following financial interests/personal relationships which may be considered as potential competing interests:

Acknowledgements

The study was partly funded by TEQIP III, UIET, Panjab University, Chandigarh.

Data sharing: The nanoparticle characterization data used to support the findings of this study are included within the article. Other data used to support the findings of this study will be available from the corresponding author upon request.

References

[1] Y. Liu, S. Wang, Z. Wang, N. Ye, H. Fang, D.-G. Wang, TiO_2, SiO_2 and ZrO_2 nanoparticles synergistically provoke cellular oxidative damage in freshwater microalgae, Nanomater. (Basel, Switzerland) 8 (2018).

[2] R. Yu, J. Wu, M. Liu, L. Chen, G. Zhu, H. Lu, Physiological and transcriptional responses of Nitrosomonas europaea to TiO_2 and ZnO nanoparticles and their mixtures, Environ. Sci. Pollut. Res. 23 (2016).

[3] M. Tsugita, N. Morimoto, M. Nakayama, SiO_2 and TiO_2 nanoparticles synergistically trigger macrophage inflammatory responses, Part. Fibre Toxicol. 14 (April (1)) (2017) 11.

[4] T. Tong, et al., Combined toxicity of nano-ZnO and Nano-TiO_2: from single- to multinanomaterial systems, Environ. Sci. Technol. 49 (13) (2015) 8113–8123.

[5] J. Hua, W.J.G.M. Peijnenburg, M.G. Vijver, TiO_2 nanoparticles reduce the effects of ZnO nanoparticles and Zn ions on zebrafish embryos (Danio rerio), NanoImpact 2 (2016) 45–53.

[6] E. Salih, M. Mekawy, R.Y.A. Hassan, I.M. El-Sherbiny, Synthesis, characterization and electrochemical-sensor applications of zinc oxide/graphene oxide nanocomposite, J. Nanostruct. Chem. 6 (June (2)) (2016) 137–144.

[7] Z. Durmus, B.Z. Kurt, A. Durmus, Synthesis and characterization of graphene oxide/zinc oxide (GO/ZnO) nanocomposite and its utilization for photocatalytic degradation of basic Fuchsin dye, ChemistrySelect 4 (1) (2019) 271–278.

[8] V.R. Posa, V. Annavaram, J.R. Koduru, V.R. Ammireddy, A.R. Somala, Graphene-ZnO nanocomposite for highly efficient photocatalytic degradation of methyl orange dye under solar light irradiation, Korean J. Chem. Eng. 33 (2) (2016) 456–464 Feb.

[9] J. Wang, T. Tsuzuki, B. Tang, X. Hou, L. Sun, X. Wang, Reduced graphene Oxide/ZnO composite: reusable adsorbent for pollutant management, ACS Appl. Mater. Interfaces 4 (6) (2012) 3084–3090.

[10] S. Xu, L. Fu, T.S.H. Pham, A. Yu, F. Han, L. Chen, Preparation of ZnO flower/reduced graphene oxide composite with enhanced photocatalytic performance under sunlight, Ceram. Int. 41 (Part A (3)) (2015) 4007–4013.

[11] J. Jayachandiran, et al., Synthesis and electrochemical studies of rGO/ZnO nanocomposite for supercapacitor application, J. Inorg. Organomet. Polym. Mater. 28 (5) (2018) 2046–2055 Sep.

[12] N. Ye, Z. Wang, S. Wang, W.J.G.M. Peijnenburg, Toxicity of mixtures of zinc oxide and graphene oxide nanoparticles to aquatic organisms of different trophic level: particles outperform dissolved ions, Nanotoxicology 12 (5) (2018) 423–438.

[13] B. Wu, et al., Combined effects of graphene oxide and zinc oxide nanoparticle on human A549 cells: bioavailability{,} toxicity and mechanisms, Environ. Sci. Nano 6 (2) (2019) 635–645.

[14] C. Chung, Y.-K. Kim, D. Shin, S.-R. Ryoo, B.H. Hong, D.-H. Min, Biomedical applications of graphene and graphene oxide, Acc. Chem. Res. 46 (10) (2013) 2211–2224.

[15] A. Kołodziejczak-Radzimska, T. Jesionowski, A. Krysztafkiewicz, Obtaining zinc oxide from aqueous solutions of KOH and $Zn(CH_3COO)_2$, Physicochem. Probl. Miner. Process. 44 (2010) 93–102.

[16] Y. Zheng, R. Li, Y. Wang, In vitro and in vivo biocompatibility studies of Zno nanoparticles, Int. J. Mod. Phys. B 23 (2009) 1566–1571.

[17] C. Mihai, et al., Intracellular accumulation dynamics and fate of zinc ions in alveolar epithelial cells exposed to airborne ZNO nanoparticles at the air-liquid interface, Nanotoxicology 9 (2013).

[18] H. Attia, H. Nounou, M. Shalaby, Zinc oxide nanoparticles induced oxidative DNA damage, inflammation and apoptosis in rat's brain after oral exposure, Toxics 6 (2018) 29.

[19] L. Tian, et al., Neurotoxicity induced by zinc oxide nanoparticles: age-related differences and interaction, Sci. Rep. 5 (2015) 16117.

[20] W. Zhang, S. Bao, T. Fang, The neglected nano-specific toxicity of ZnO nanoparticles in the yeast Saccharomyces cerevisiae, Sci. Rep. 6 (2016) 24839.

[21] L. Ou, et al., Toxicity of graphene-family nanoparticles: a general review of the origins and mechanisms, Part. Fibre Toxicol. 13 (October (1)) (2016) 57.

[22] O. Akhavan, E. Ghaderi, Toxicity of graphene and graphene oxide nanowalls against Bacteria, ACS Nano 4 (10) (2010) 5731–5736.

[23] L. De Marzi, et al., Flake size-dependent cyto and genotoxic evaluation of graphene oxide on in vitro A549, CaCo2 and Vero cell lines, J. Biol. Regul. Homeost. Agents 28 (2014).

[24] P. Ray, H. Yu, P.P. Fu, Toxicity and environmental risks of nanomaterials: challenges and future needs, J. Environ. Sci. Health C Environ. Carcinog. Ecotoxicol. Rev. 27 (2009) 1–35.

[25] A. Picado, et al., Strategic Management and Assessment of Risks and Toxicity of Engineered Nanomaterials, (2009), pp. 95–109.

[26] R. Chakraborty, et al., Characterization of a Drosophila Alzheimer's disease model: pharmacological rescue of cognitive defects, PLoS One 6 (6) (2011) 1–13.

[27] J. Botella, F. Bayersdorfer, F. Gmeiner, S. Schneuwly, Modelling Parkinson's disease in Drosophila, Neuromol. Med. 11 (2009) 268–280.

[28] A. Abolaji, D.J.P. Kamdem, O. Farombi, J.B. Rocha, *Drosophila melanogaster* as a promising model organism in toxicological studies: a mini review, Arch. Basic Appl. Med. 1 (2013) 33–38.

[29] D.C. Marcano, et al., Improved synthesis of graphene oxide, ACS Nano 4 (8) (2010) 4806–4814.

[30] A. Gopal, A simple approach to stepwise synthesis of graphene oxide nanomaterial, J. Nanomed. Nanotechnol. 6 (2015) 1000253.

[31] D. Gnanasangeetha, T.D. Sarala, One pot synthesis of zinc oxide nanoparticles via chemical and green method, Int. Res. J. Mater. Sci. Appl. 1 (2013) 1–8.

[32] P. Eslin, G. Prévost, Hemocyte load and immune resistance to *Asobara tabida* are correlated in species of the *Drosophila melanogaster* subgroup, J. Insect Physiol. 44 (9) (1998) 807–816.

[33] C. Nichols, J. Becnel, U. Pandey, Methods to assay Drosophila behavior, J. Vis. Exp. 61 (2012).

[34] F. Wolf, A. Rodan, L.T. Tsai, U. Heberlein, High-resolution analysis of ethanol-induced locomotor stimulation in Drosophila, J. Neurosci. 22 (2002) 11035–11044.

[35] C. Wojcik, G.N. DeMartino, Analysis of Drosophila 26 S proteasome using RNA interference, J. Biol. Chem. 277 (2002) 6188–6197.

[36] M. Beltramí, M. Cristina Medina Muñoz, D. Arce, R. Godoy-Herrera, Drosophila pupation behavior in the wild, Evol. Ecol. 24 (2010).

[37] M. Cristina Medina-Muñoz, R. Godoy-Herrera, Dispersal and prepupation behavior of Chilean sympatric Drosophila species that breed in the same site in nature, Behav. Ecol. 16 (2005) 316–322.

[38] A. Joshi, L. Mueller, Directional and stabilizing density-dependent natural selection for pupation height in *Drosophila melanogaster*, Evolution (N. Y) 47 (1993) 176.

[39] M.M. Bradford, A rapid and sensitive method for the quantitation of microgram quantities of protein utilizing the principle of protein-dye binding, Anal. Biochem. 72 (1) (1976) 248–254.

[40] Y. Siddique, et al., Toxic potential of synthesized graphene zinc oxide nanocomposite in the third instar larvae of transgenic Drosophila melanogaster (hsp70-lacZ)Bg9, Biomed Res. Int. 2014 (2014) 382124.

[41] S.S. Kumar, P. Venkateswarlu, V.R. Rao, G.N. Rao, Synthesis, characterization and optical properties of zinc oxide nanoparticles, Int. Nano Lett. 3 (1) (2013) 30 May.

[42] B. Baruwati, D.K. Kumar, S.V. Manorama, Hydrothermal synthesis of highly crystalline ZnO nanoparticles: a competitive sensor for LPG and EtOH, Sens. Actuators B

Chem. 119 (2) (2006) 676–682.
[43] D. Li, M.B. Müller, S. Gilje, R. Kaner, G. Wallace, Processable aqueous dispersion of graphene nanosheets, Nat. Nanotechnol. 3 (2008) 101–105.
[44] X. Gao, J. Jang, S. Nagase, Hydrazine and thermal reduction of graphene oxide: reaction mechanisms, product structures, and reaction design, J. Phys. Chem. C 114 (2) (2010) 832–842.
[45] Interpretation of Infrared Spectra, *UMass Boston OpenCourseWare*, (2008) Available: http://ocw.umb.edu/chemistry/organic-chemistry-i-lecture/lecture-links/notes92208.pdf . (Accessed 26 September 2018).
[46] R. Zamiri, A. Zakaria, H. Ahangar, M. Darroudi, A. Khorsand Zak, G. Drummen, Aqueous starch as a stabilizer in zinc oxide nanoparticle synthesis via laser ablation, J. Alloys. Compd. 516 (2012) 41–48.
[47] S. Kumar, A. Kandasami, R. Singh, S. Chatterjee, D. Kanjilal, A. Ghosh, Investigations on structural and optical properties of ZnO and ZnO:Co nanoparticles under dense electronic excitations, RSC Adv. 4 (2014).
[48] S. Tyagi, A. Arya, P.K. Tyagi, S. Singh, Development of *Drosophila melanogaster* for assessing metal nanoparticles interaction, Int. J. Basic Appl. Biol. 3 (2) (2016) 132–135.
[49] M.B. Sokolowski, Genetics and ecology of *Drosophila melanogaster* larval foraging and pupation behaviour, J. Insect Physiol. 31 (11) (1985) 857–864.
[50] M. Khatri, et al., Evaluation of cytotoxic, genotoxic and inflammatory responses of nanoparticles from photocopiers in three human cell lines, Part. Fibre Toxicol. 10 (2013) 42.
[51] J. Kaur, M. Khatri, S. Puri, Toxicological evaluation of metal oxide nanoparticles and mixed exposures at low doses using zebra fish and THP1 cell line, Environ. Toxicol. 34 (4) (2019) 375–387.
[52] I.-L. Hsiao, Y.-J. Huang, Effects of various physicochemical characteristics on the toxicities of ZnO and TiO_2 nanoparticles toward human lung epithelial cells, Sci. Total Environ. 409 (7) (2011) 1219–1228.
[53] G. Oberdörster, E. Oberdörster, J. Oberdörster, Nanotoxicology: an emerging discipline evolving from studies of ultrafine particles, Environ. Health Perspect. 113 (2005) 823–839.
[54] A. Nel, T. Xia, L. Mädler, N. Li, Toxic potential of materials at the nanolevel, Science 311 (2006) 622–627.
[55] K. Powers, S. Brown, V. Krishna, S. Wasdo, B. Moudgil, S.M. Roberts, Research strategies for safety evaluation of nanomaterials. Part VI. Characterization of nanoscale particles for toxicological evaluation, Toxicol. Sci. 90 (2006) 296–303.
[56] Y. Chang, et al., In vitro toxicity evaluation of graphene oxide on A549 cells, Toxicol. Lett. 200 (3) (2011) 201–210.